Journal of Biomechanics 104 (2020) 109711

Contents lists available at ScienceDirect

Journal of Biomechanics

journal homepage: www.elsevier.com/locate/jbiomech
www.JBiomech.com

Whole-body dynamic stability in side cutting: Implications for markers of lower limb injury risk and change of direction performance

Sean P. Sankey [a,b,*], Mark A. Robinson [a], Jos Vanrenterghem [c]

[a] Research Institute for Sport and Exercise Sciences, Faculty of Science, Liverpool John Moores University, Liverpool, UK
[b] School of Sport and Biological Sciences, University of Bolton, Bolton, UK
[c] KU Leuven, Musculoskeletal Rehabilitation Research Group, Department of Rehabilitation Sciences and Physiotherapy, Faculty of Kinesiology and Rehabilitation Sciences, Belgium

ARTICLE INFO

Article history:
Accepted 18 February 2020

Keywords:
Centre of mass
Dynamic stability
Side cutting
Anterior cruciate ligament
Sagittal plane efficiency

ABSTRACT

Control of the centre of mass (CoM) whilst minimising the use of unnecessary movements is imperative for successful performance of dynamic sports tasks, and may indicate the condition of *whole-body dynamic stability*. The aims of this study were to express movement strategies that represent whole-body dynamic stability, and to explore their association with potentially injurious joint mechanics and side cutting performance. Twenty recreational soccer players completed 45° unanticipated side cutting. Five distinct whole-body dynamic stability movement strategies were identified, based on factors that influence the medial ground reaction force (GRF) vector during ground contact in the side cutting manoeuvre. Using Statistical Parametric Mapping, the movement strategies were linearly regressed against selected performance outcomes and peak knee abduction moment (peak KAM). Significant relationships were found between each movement strategy and at least one selected performance outcome or peak KAM. Our results suggest excessive medial GRFs were generated through sagittal plane movement strategies, and despite being beneficial for performance aspects, poor sagittal plane efficiency may destabilise control of the CoM. Frontal plane hip acceleration is the key non-sagittal plane movement strategy used in a corrective capacity to moderate excessive medial forces. However, whilst this movement strategy offered a way to retrieve control of the CoM, mitigating reduced whole-body dynamic stability, it also coincided with increased peak KAM. Overall, whole-body dynamic stability movement strategies helped explain the delicate interplay between the mechanics of changing direction and undesirable joint moments, providing insights that might support development of future intervention strategies.

1. Introduction

Control of the centre of mass (CoM) is prioritised above all other demands in dynamic movement (MacKinnon and Winter, 1993; Patla et al., 1999). When CoM control is lost, we may observe a fall, failure to execute the task, or a scenario where excessive stress is placed on the musculoskeletal system to prevent either of those from happening. To avoid a fall or a failure of the task one may exhibit undesirable deviations in technique that may be a precursor to dangerous joint loading. The influence of controlled technique changes in side cutting has been explored in the context of Anterior Cruciate Ligament (ACL) injury risk by several research groups (Dempsey et al., 2009; Donnelly et al., 2012; Kristianslund et al., 2014; Havens and Sigward, 2015a; 2015b; 2015c; Jones et al., 2015; David et al., 2017). However, it is often not clear how common kinematic and kinetic variables are associated with each other toward general control of the CoM, or even how their roles may change through phases of ground contact. Donnelly et al. (2012) used biomechanical simulations to suggest that redirecting the whole-body CoM medially and towards the direction of travel would bring about a reduced external peak knee abduction moment (KAM). Whilst this is important for ACL injury risk, it is unclear through which movement strategies such a redirection of the CoM could best be achieved without causing task failure or increased stresses elsewhere in the musculoskeletal system. Currently, this makes it difficult for a practitioner to interpret findings towards meaningful intervention strategies. Therefore, a more holistic view of the movement strategies that are necessary in control of the CoM may highlight the condition of whole-body dynamic stability, and the intricate interplay between task performance and injury risk.

Side cutting involves generating an impulse against the ground to decelerate then accelerate the CoM. In addition to the approaching velocity, it is specifically the accelerative impulse in the medial

* Corresponding author at: School of Sport and Biological Sciences, University of Bolton, Bolton, UK.
E-mail address: S.Sankey@bolton.ac.uk (S.P. Sankey).

https://doi.org/10.1016/j.jbiomech.2020.109711
0021-9290/

direction that determines the actual change of direction of the CoM and acceleration in the new direction of travel – i.e. task performance. Detailed expression of factors that influence the medial ground reaction force (GRF) vector may therefore quantify how these important impulses are generated, and thus, the movement strategies that are important for medial control of the CoM. To begin to quantify the medial GRF vector, we must start with where the foot is placed. It is possible to quantify foot placement by the dynamic association between the CoM and base of support, similar to the margin of stability previously reported (Hof et al., 2005; Havens et al., 2018). In this case, foot placement also represents an initial condition of whole-body dynamic stability within the task. Once the foot is placed, the origin of the GRF vector is the centre of pressure (CoP) under the foot. Although the CoP is limited to the boundaries of the base of support, the CoP position may change over ground contact time, perhaps in response to ankle movement. Subsequently, we can attempt to express the magnitude of the medial GRF vector, but more importantly, the contribution of the individual joint moments. Whilst joint contributions are rather elusive and difficult to quantify independently, the application of Induced Acceleration Analysis (IAA) may offer a useful approach.

Previous research has demonstrated the possibility of using IAA modelling to estimate the relative contribution of lower limb joint moments to GRF components (Kepple et al., 1997; João et al., 2014; Moniz-Pereira et al., 2018). Following calculation of the joint positions and net joint moments of the lower limb, the equations of motion can be solved, computing the relative contribution of each moment to accelerate the CoM (João et al., 2014). Thus, due to the direct relationship with acceleration of the CoM and GRF, one can express the relative contribution of each joint moment to the medial component of the GRF, for example. Once the factors that influence GRF vector are quantified, it is possible to determine their association with selected performance outcome and undesirable joint loading variables.

Therefore, key movement strategies for medial control of the CoM in side cutting are quantified through factors that influence the medial GRF vector, and this is likely to offer an integrated account of performance and injury risk. The aims of this study were to outline key mechanical movement strategies, specifically exploring their role in enhancing CoM change of direction angle and acceleration, whilst minimising peak KAM. As fulfilling these roles are likely to be disparate, this provides a unique challenge to the key movement strategies. Thus, it is hypothesised that movement strategies necessary to increase change of direction angle and acceleration, will also increase peak KAM.

2. Methods

2.1. Participants

The participants in this study were twenty healthy male recreational soccer players, with at least 6 years playing experience. The participants had a mean (±SD) age of 23 ± 3 years; mean height of 1.8 ± 0.1 m; and mean mass of 76.7 ± 10.4 kg. All participants were free from injury for at least 6 months, and written consent was retrieved from every participant. All participant recruitment processes were conducted in line with the university research ethics committee guidelines, which comply with the principles of the Declaration of Helsinki.

2.2. Protocol – side cutting assessment

Mock testing conditions were simulated in a familiarisation session no more than one week before the testing session. In the testing session, participants first completed a dynamic warm-up, as well as specific side cutting practice. Participants then completed a static trial and functional hip joint centre and knee joint axis tasks in the centre of the capture volume. Following calibration trials the motion trials were collected. The unanticipated side cutting task was controlled with a 4–5 m s^{-1} approach velocity, using timing gates (Smartspeed™, Fusion Sports, Australia) set 2 m apart, at 5 m and 3 m away from the force plate. The 45° change with respect to forward progression was marked out to the left and right from the force platform with the use of cones. The preferred leg for change of direction was used for all trials meaning participants completed either side cutting or cross-over cutting depending on the light stimulus they received. To trigger the direction of onward progression, the light stimulus appeared on either the left or right, and participants were told to cut in the direction of the light (see Appendix A). The cueing light units to indicate the direction of the two unanticipated conditions were set up 3 m beyond the force plate, 1 m in height from the ground, and 2 m apart. If participants failed to adhere to the path or velocity constraints set for the side cutting task, that trial was discarded, and an additional trial was added to the trial count. On average the participants completed 24 trials in total, 12 side cutting and 12 cross-over cutting trials, subsequently, the participants completed a 10–15 min cool-down protocol.

2.3. Biomechanical model

All participants had 44 reflective markers captured based on the Liverpool John Moores University Lower Limb and Trunk eight segment model (Vanrenterghem et al., 2010). Markers were applied to participants before a 15-minute dynamic warm-up, and bandages and strapping used to attach cluster plates on lower limb segments were adjusted for comfort, without compromising a secure fitting. 3D marker trajectory data were recorded using a 7-camera Vicon MX system (Vicon, Oxford Metrics, Oxford, UK) at 250 Hz for the side cutting motion trials. Joint centres, axes and local segment coordinate systems were defined as reported previously (Vanrenterghem et al., 2010). The side cutting tasks were executed on a 0.6 × 0.4 m force platform (Kistler, Winterthur, Switzerland), and force data were sampled at 1500 Hz and synchronised with the Vicon system. Calibration, modelling, and all kinematic and kinetic analyses were completed in Visual 3D Professional (v.5.00.16, C-Motion, Germantown, MD, USA), and were based on segmental data from Dempster's regression equations (Dempster, 1955), moment of inertia properties from Hanavan (1964), and the use of geometric volumes to represent each of the eight segments. Inverse kinematic (IK) modelling was used in Visual 3D as a pre-requisite for IAA.

2.4. Data processing

Only the side cutting trials were analysed. Marker coordinate data and analogue signals from the force plate channels were filtered using a Butterworth 4th order recursive low pass filter, with a 20 Hz cut-off frequency (Kristianslund et al., 2012). Following IK modelling, inverse dynamics calculations were used to estimate the net external joint moments (cardan sequence – X-Y-Z). Touchdown (TD) and toe-off (TO) events were calculated as reported previously (Vanrenterghem et al., 2012; Sankey et al., 2015) to determine the ground contact phase. The CoM transverse plane trajectory angle and velocity were calculated. *Change of direction angle* was calculated as the change in CoM trajectory angle between TD and TO. Changes in M-L CoM velocity, once divided by ground *contact time*, represented the *average medial CoM acceleration* from TD to TO. Change of direction angle and average medial CoM acceleration were used to represent two selected performance outcomes. *Peak KAM* relative to body mass was

calculated over the *weight acceptance phase* according to previous research (Besier et al., 2001), and was found to be 0–23% ground contact, on average, in the present study.

2.5. Quantification of whole-body dynamic stability

Factors that influence the medial GRF vector were calculated to represent whole-body dynamic stability. The first priority was to calculate foot placement, which would influence the origin of the GRF vector, and represents the dynamic relationship between the CoM and base of support. Firstly, the 'extrapolated' CoM (XCoM) was calculated according to Hof (2008) (see Eq. (1)).

$$\mathrm{XCoM} = \mathrm{pCoM} + \frac{\mathrm{vCoM}}{\sqrt{\mathrm{gl}^{-1}}} \quad (1)$$

where *pCoM* is the M-L position of the CoM, *vCoM* is the M-L velocity of the CoM, *g* is gravity, and *l* is the distance between the CoM and ankle in the frontal plane. The first whole-body dynamic stability variable – (1) M-L *foot placement* – was calculated as the position of the XCoM relative to the fifth metatarsal head (MTH5) which was indicative of the lateral border of the foot. In this case, a positive value for foot placement would indicate the XCoM is medial to the planted foot, whilst a negative value would indicate the XCoM is lateral and considered outside of the base of support. The second variable – (2) *position of the CoP* – was calculated as the origin of the GRF vector under the planted foot – again, measured relative to MTH5, but unlike foot placement position of the CoP was measured across ground contact.

IAA modelling, explained in detail elsewhere (Kepple et al., 1997; João et al., 2014; Moniz-Pereira et al., 2018), was conducted in Visual 3D to determine all non-negligible (>10 N) contributions to the medial GRF. Non-negligible contributions to the M-L GRFs were found in sagittal plane hip, knee and ankle joints, and also in the frontal and transverse planes for the hip joint. Those contributions were then consolidated in their respective planes to represent the third, fourth, and fifth whole-body dynamic stability movement strategies: (3) *Sagittal triple acceleration* (the sum of the sagittal plane hip, knee and ankle joint contributions); (4) *frontal plane hip acceleration*; (5) *transverse plane hip acceleration* (see Fig. 1 diagram). Following previous research (Kepple et al., 1997; João et al., 2014; Moniz-Pereira et al., 2018) the error of IAA was determined by finding the absolute mean difference of CoM acceleration from the force plate ground reaction forces and those derived from the sum of all joint contributions in IAA. The difference was then represented as a percentage of the maximum force obtained from the force plate - in this case the mean error for medio-lateral IAA was found to be 7%. The mean error in the

Table 1
Side cutting performance outcome variables and peak knee abduction moment - means are presented with standard deviations (*SD*).

Performance outcome/joint loading variable	Unanticipated side cutting
Touchdown Velocity (ms^{-1})	3.95
±*SD*	*0.30*
Toe-off Velocity (ms^{-1})	4.00
±*SD*	*0.24*
Change of direction angle (°)	20.6
±*SD*	*3.2*
Average medial CoM acceleration (ms^{-2})	4.91
±*SD*	*0.91*
Contact time (s)	0.28
±*SD*	*0.03*
Peak KAM (Nm/kg)	0.44
±*SD*	*0.25*

* 'CoM' denotes centre of mass; 'KAM' denotes knee abduction moment.

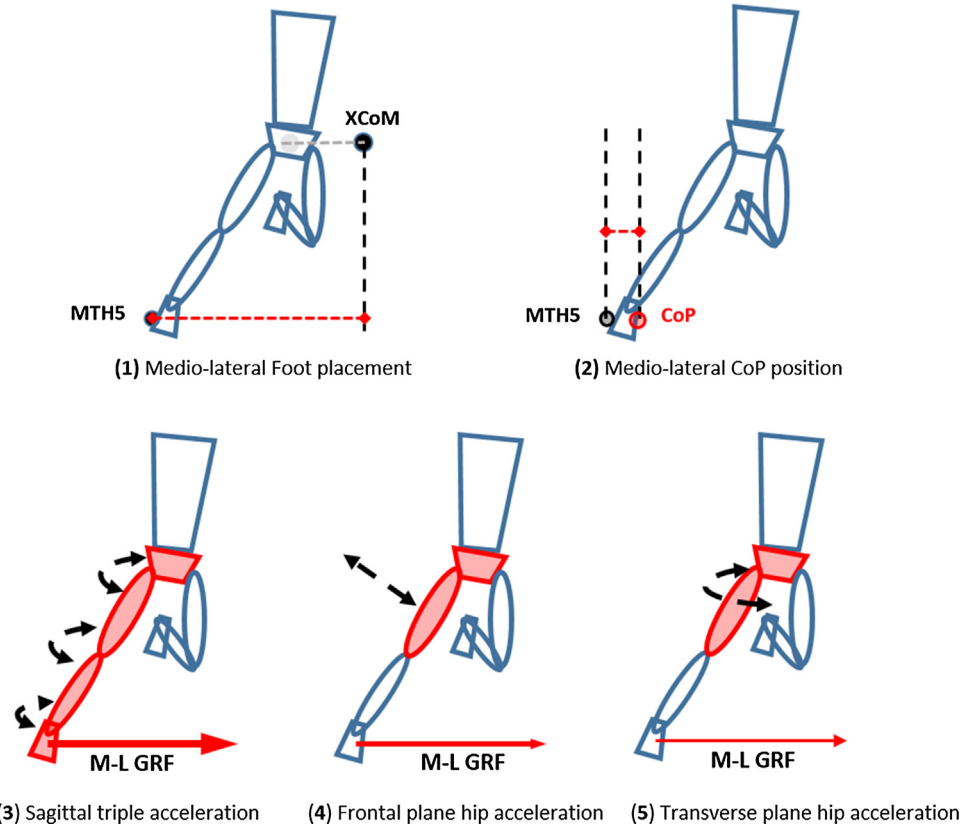

Fig. 1. Diagram of the five distinct whole-body dynamic stability movement strategies for medio-lateral control of the CoM.

Table 2
Summary of general findings of the multiple linear regression analyses conducted in SPM1D. The significance of each regression between pairs of variables is presented, and when p < 0.003 the direction of the relationship is also presented in parenthesis ('−ve' = variables have a negative relationship; '+ve' = variables have a positive relationship).

Whole-body dynamic Stability variables	Selected performance outcome and joint loading variables		
	Average medial CoM acceleration (TD-TO) ^{0D}	Change of direction angle (TD-TO) ^{0D}	Peak KAM (weight acceptance phase) ^{0D}
(1) Foot placement ^{0D}	p = 0.008	p = 0.001* (−ve)	p = 0.001* (−ve)
(2) M-L Centre of Pressure (CoP) position ^{1D}	p < 0.003* (−ve)	p = 0.001* (−ve)	p > 0.003
(3) Sagittal triple acceleration ^{1D}	p < 0.003* (+ve)	p < 0.003* (+ve)	p < 0.003*(+ve)
(4) Frontal plane hip acceleration ^{1D}	p > 0.003	p < 0.003* (+ve)	p < 0.003* (+ve)
(5) Transverse plane hip acceleration ^{1D}	p > 0.003	p < 0.003* (+ve)	p < 0.003* (+ve)

'*' = significance (α = 0.003); '^{0D}' = 0-dimensional data; '^{1D}' = 1-dimensional (time-series) continua. Beta regression data are presented in Appendix B for mechanism 1, and single subject examples are presented in the second column in Figs. 2–5 for mechanisms 2–5.

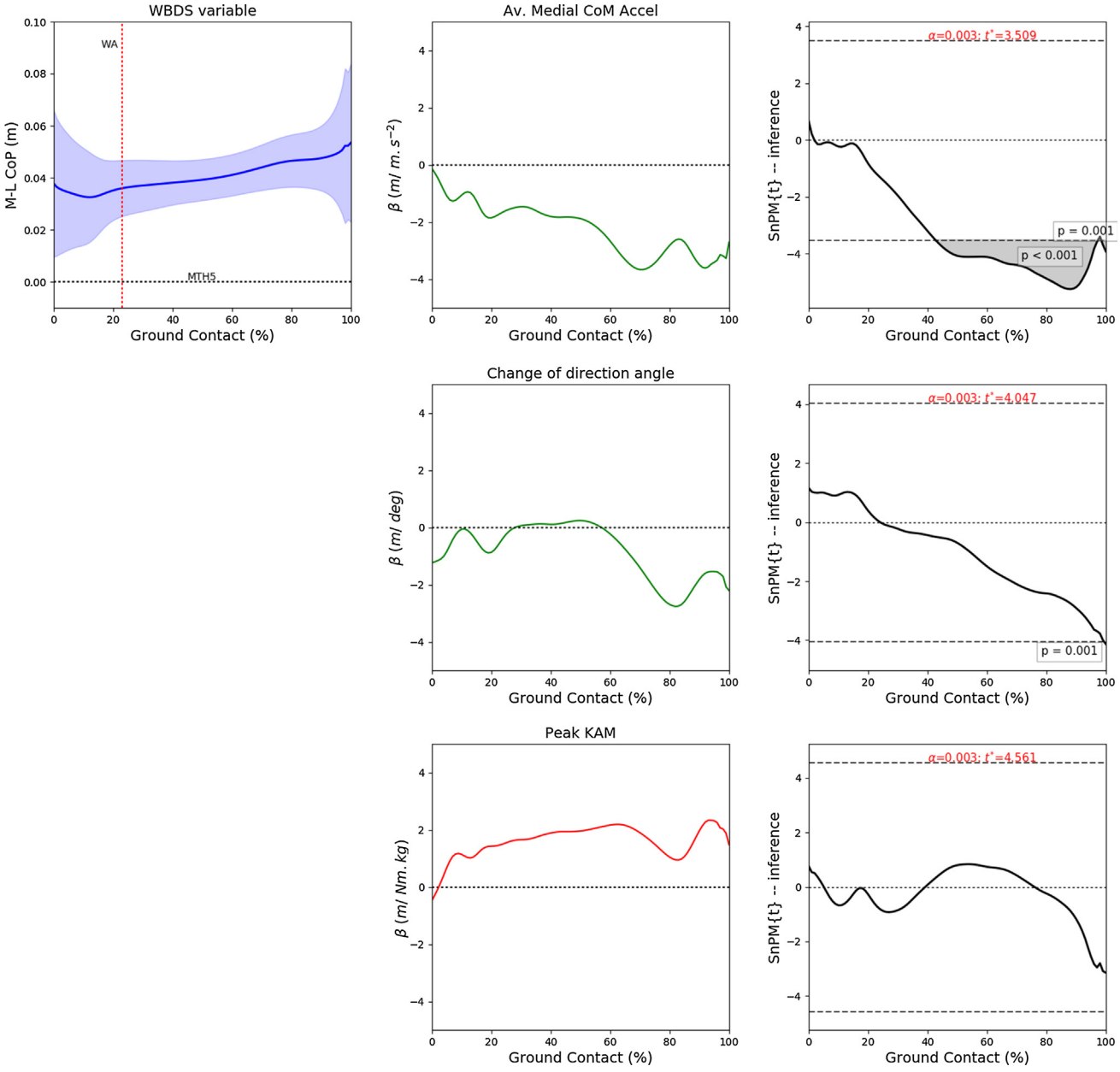

Fig. 2. Characterisation of the relationship between whole-body dynamic stability (WBDS) variable *M-L CoP position* and average medial CoM acceleration, change of direction angle, and peak knee abduction moment (Peak KAM). Row 1, column 1 shows the mean and standard deviation of the time-series M-L *CoP position* signals, lateral border of the foot is represented by dotted line and label at position '0.00' on the y-axis highlighting the position of metatarsal head 5 (MTH5); weight acceptance (WA) is indicated by the vertical line at 23% ground contact. Row 1 column 2 shows the beta curves in regression against average medial CoM acceleration; then the row 1 column 3 shows the one sample *t*-test statistical curve (SnPM{t}), where α = 0.003, with inference boundaries and p values for significance clusters, where applicable. Columns 2 and 3 are repeated for change of direction angle and Peak KAM on rows 2 and 3, respectively. Example beta regression curves are presented in column 2: green for selected performance outcomes, and red for peak KAM. (For interpretation of the references to colour in this figure legend, the reader is referred to the web version of this article.)

current study is comparable to the 4.8% and 5.4% mean vertical error reported for stair ambulation and hopping tasks, respectively.

2.6. Statistical analysis

Following normality tests, we ran Pearson's correlations for participant mass, height, and touchdown speed against our selected performance outcomes and peak KAM (IBM SPSS Statistics, v23, Chicago, USA). This allowed us to investigate the impact of typical sources of between-individual (inter-individual) variability that may remain within the boundaries of the side cutting task exclusion criteria. Subsequently, all further statistical analyses were computed in SPM1D (v0.4, www.spm1d.org) using Python (Python v2.7.1 Enthought Canopy, v1.6.2, Enthought Python Distribution, Austin, TX, USA), and using Statistical Parametric Mapping (SPM) (Pataky, 2012) for regressions involving 1D time-series data.

Using SPM1D, non-parametric linear regression analyses were computed to investigate within-individual (intra-individual) variations in task execution. The regression analyses were similar to that previously reported (Vanrenterghem et al., 2012). Fifteen linear regression analyses were conducted for each combination of the three 0D independent variables – change of direction angle, average M-L CoM acceleration and peak KAM – regressed against the five whole-body dynamic stability dependent variables. Alpha

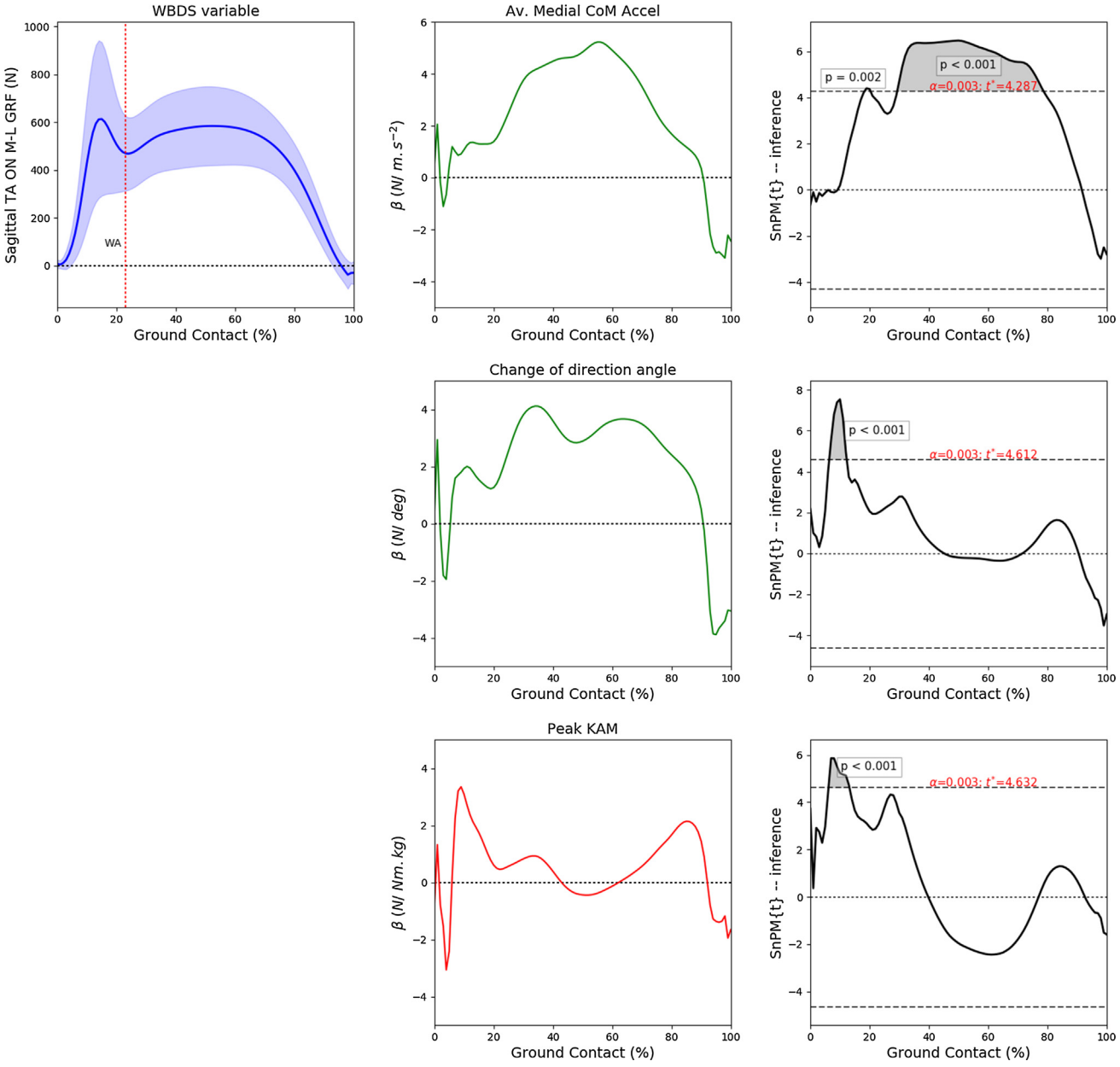

Fig. 3. Characterisation of the relationship between whole-body dynamic stability (WBDS) variable *sagittal triple acceleration (TA)* contribution to M-L GRF and average medial CoM acceleration, change of direction angle, and peak knee abduction moment (Peak KAM). Row 1, column 1 shows the mean and standard deviation of the time-series Sagittal TA signals; weight acceptance (WA) is indicated by the vertical line at 23% ground contact. Row 1 column 2 shows the beta curves in regression against average medial CoM acceleration; then the row 1 column 3 shows the one sample *t*-test statistical curve (SnPM{t}), where $\alpha = 0.003$, with inference boundaries and p values for significance clusters, where applicable. Columns 2 and 3 are repeated for change of direction angle, then Peak KAM on rows 2 and 3, respectively. Example beta regression curves are presented in column 2: green for selected performance outcomes, and red for peak KAM. (For interpretation of the references to colour in this figure legend, the reader is referred to the web version of this article.)

was adjusted *a priori* from $\alpha = 0.05$ to $\alpha = 0.003$, using a Bonferroni correction based on the number of variables.

In further analysis, we noted that it may be possible to represent the extent of the sagittal and non-sagittal contributions to change of direction in a single metric, which may be a useful reference for practitioners when monitoring effectiveness of intervention strategies. To quantify this observation specifically, we calculated the sagittal triple acceleration impulse and total M-L force impulse, and expressed the former as a percentage of the latter, representing a *Sagittal Efficiency Ratio*. A *Sagittal Efficiency Ratio* of 100% would mean the impulses were equal and the medial CoM acceleration was entirely sagittal. However, lower or higher than 100% would mean non-sagittal movements were involved in generating (increasing) or moderating (reducing) medial CoM acceleration, respectively.

3. Results

On average, the resultant CoM velocity at touchdown was slightly lower than the required 4–5 ms^{-1} threshold, followed by a small increase in velocity by toe-off (see Table 1). The change of direction angle was also below the intended 45° at 20.6°, on average (see Table 1). No significant correlations were found between participant mass, height, and approach speed, and the selected performance outcomes or peak KAM.

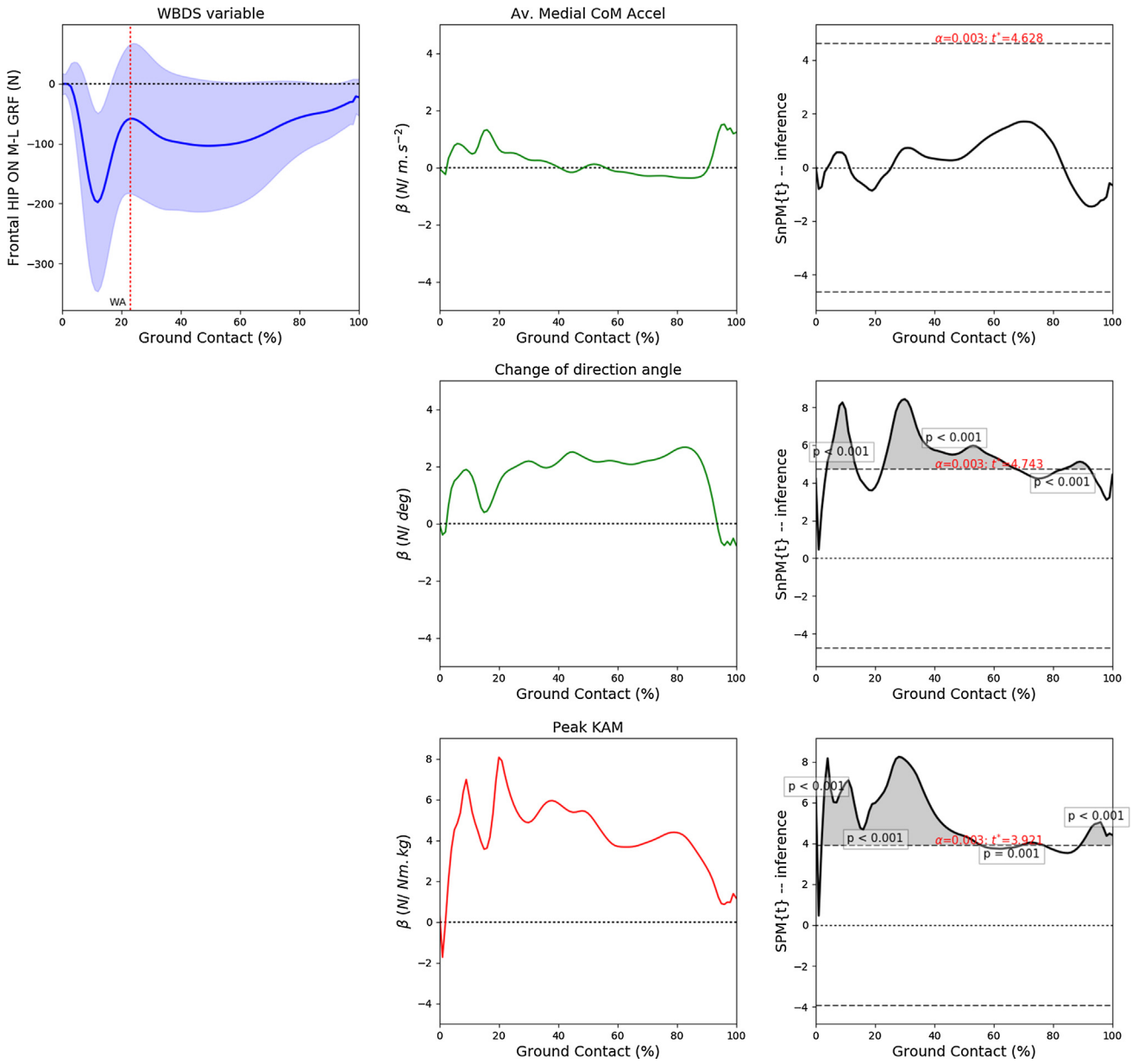

Fig. 4. Characterisation of the relationship between whole-body dynamic stability (WBDS) variable *frontal plane hip acceleration* contribution to M-L GRF and average medial CoM acceleration, change of direction angle, and peak knee abduction moment (Peak KAM). Row 1, column 1 shows the mean and standard deviation of the time-series frontal plane hip acceleration signals; weight acceptance (WA) is indicated by the vertical line at 23% ground contact. Row 1 column 2 shows the beta curves in regression against average medial CoM acceleration; then the row 1 column 3 shows the one sample *t*-test statistical curve (SnPM{t}), where $\alpha = 0.003$, with inference boundaries and p values for significance clusters, where applicable. Columns 2 and 3 are repeated for change of direction angle, then Peak KAM on rows 2 and 3, respectively. Example beta regression curves are presented in column 2: green for selected performance outcomes, and red for peak KAM. (For interpretation of the references to colour in this figure legend, the reader is referred to the web version of this article.)

In the 15 regression outputs, negative betas indicated negative relationships, whilst positive betas indicate positive relationships between the independent and dependent variables. The average foot placement was found to be 0.428 ± 0.059 m representing the medial distance from the MTH5, on the lateral border of the foot, to the XCoM. A narrower foot placement (see Table 2), followed by a more lateral position of the CoP during contact, seems to increase average medial CoM acceleration and change of direction angle to a lesser extent (see Fig. 2). However, our findings suggest a narrower foot placement in particular, may also lead to greater peak KAM (see Table 2).

Increases in *sagittal triple acceleration*, *frontal plane hip acceleration* and *transverse plane hip acceleration* are all related to a greater change of direction angle, however, this is at the expense of increased undesirable joint moments (see Table 2 and Figs. 3–5). An increase in *sagittal triple acceleration* aligns with increases in average medial CoM acceleration, which was more pronounced later in ground contact. The positive relationship between frontal plane hip acceleration and change of direction angle was observed despite the fact that this strategy appears to be almost exclusively for creating lateral, or unloading, ground reaction forces (see Fig. 4). Transverse plane hip acceleration appears to alternate between a loading and unloading role through medial then lateral ground reaction forces over ground contact (see Fig. 5). The contribution to medio-lateral forces from sagittal triple acceleration were typically in excess of total medio-lateral forces over ground

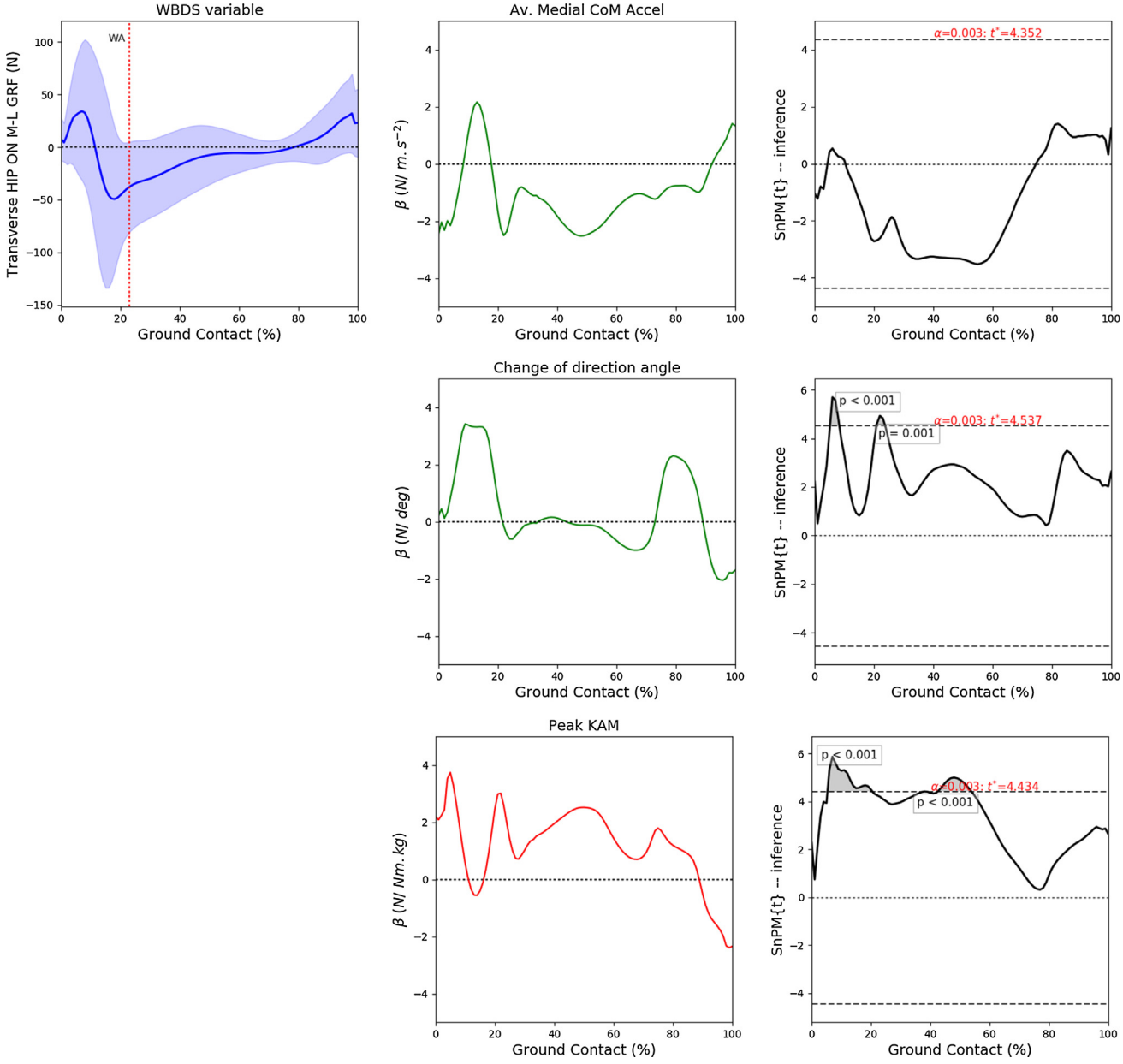

Fig. 5. Characterisation of the relationship between whole-body dynamic stability (WBDS) variable *transverse plane hip acceleration* contribution to M-L GRF and average medial CoM acceleration, change of direction angle, and peak knee abduction moment (Peak KAM). Row 1, column 1 shows the mean and standard deviation of the time-series transverse hip acceleration signals; weight acceptance (WA) is indicated by the vertical line at 23% ground contact. Row 1 column 2 shows the beta curves in regression against average medial CoM acceleration; then the row 1 column 3 shows the one sample *t*-test statistical curve (SnPM{t}), where $\alpha = 0.003$, with inference boundaries and p values for significance clusters, where applicable. Columns 2 and 3 are repeated for change of direction angle, then Peak KAM on rows 2 and 3, respectively. Example beta regression curves are presented in column 2: green for selected performance outcomes, and red for peak KAM. (For interpretation of the references to colour in this figure legend, the reader is referred to the web version of this article.)

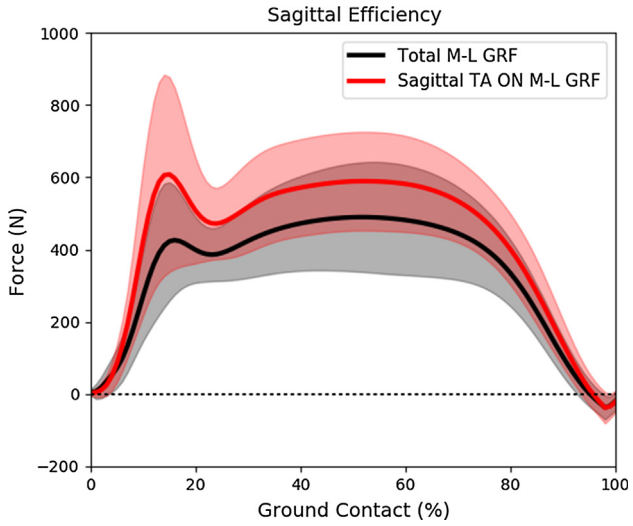

Fig. 6. Comparison of the total medio-lateral ground reaction forces (Total M-L GRF) and the sagittal triple acceleration contribution to medio-lateral ground reaction forces, estimated by induced acceleration analysis, representing Sagittal Efficiency in whole-body dynamic stability.

contact (see Fig. 6). The *Sagittal Efficiency Ratio* was 131.6 ± 30.3%, indicating that impulses from sagittal triple acceleration were excessive, on average, nearly 32% greater than the total medio-lateral impulses.

4. Discussion

The aims of this investigation were to outline mechanical movement strategies that are integral to the medial control of the CoM in side cutting, and thereby represent the condition of whole-body dynamic stability. Furthermore, we aimed to explore the influence of those specific movement strategies on redirecting and accelerating the CoM, and undesirable, potentially injurious, joint moments. Our investigation has allowed us to express systematic movement strategies that each fulfil different roles to achieve whole-body dynamic stability in unanticipated side cutting. Our findings have confirmed the hypothesis that movement strategies to increase change of direction angle and acceleration are also associated with increased peak KAM. Therefore, our findings may offer new understanding of the performance-injury trade-off in unanticipated side cutting. Specifically, we have found a narrower foot placement, along with high sagittal plane loading, are beneficial for performance aspects. However, sagittal plane strategies for generating medial forces are often excessive and inefficient, as expressed in the Sagittal Efficiency Ratio, which likely leads to destabilisation of the body. Such destabilisation requires corrective non-sagittal movement strategies and may result in higher peak KAM, and frontal plane hip acceleration appears to fulfil this important role.

The status of whole-body dynamic stability is initially determined by foot placement, and in this study a narrower foot placement may represent a more unstable initial condition (reduced medial distance from the foot to the XCoM). It has been suggested that a wider foot placement may be better for change of direction (Jones et al., 2015); however, this may not be possible in unanticipated side cutting. Furthermore, although reducing stance width may be a way to reduce harmful peak KAMs in various side cutting tasks (Dempsey et al., 2009; Kristianslund et al., 2014; Havens and Sigward, 2015a; Jones et al., 2015), our findings suggest this movement strategy is insufficient on its own for control of the CoM in unanticipated side cutting.

Following foot placement, excessive sagittal forces, as evidence by the 132% Sagittal Efficiency Ratio, risk destabilisation of the CoM, jeopardising whole-body dynamic stability and failure of the task. However, those excessive forces were moderated by frontal plane hip acceleration, which acts in countermovement to the medial forces, and more prominently so in weight acceptance. Whilst previous studies have reported the negative effects on peak KAM of a laterally flexed trunk (Dempsey et al., 2009; Jamison et al., 2012; Kristianslund et al., 2014; Jones et al., 2015), we have been able demonstrate that frontal plane hip acceleration may be the direct movement strategy at work here. Moreover, the countermovement may be necessary to control the CoM, and sufficient enough to engage the hip in transverse plane hip acceleration, which may explain a re-orientation of the pelvis. Later in ground contact, the role of hip movement strategy diminishes, and this appears to make way for an ankle movement strategy to take over. Specifically, our results suggest from ~43% ground contact a more lateral CoP position, which is likely due to inversion of the subtalar joint, increases the ability to accelerate the CoM medially. Perhaps this is evidence of a double pendulum interaction between hip and ankle movement strategies at work in the frontal plane, as previously reported for a range of tasks (MacKinnon and Winter, 1993; Winter, 1995; Houck et al., 2006).

On average participants' final approach velocity and change of direction angle was lower than expected when the CoM trajectory was analysed directly, despite participants apparently meeting the predetermined constraints at the time of data collection in the lab. However, this limitation is a frequent observation in the literature for change of direction angle (Dos'Santos et al., 2018). Observation of the preceding steps may clarify other braking characteristics; nonetheless, our findings should be interpreted in light of the mean approach velocity we reported, which was around 4 m s^{-1}. The use of IAA in decomposition of movement dynamics continues to be a source of some debate (Chen, 2006; João et al., 2014), which is beyond the scope of this study. However, we feel this approach offers important insights into mechanics in the kinetic chain, and we have provided a calculation of the error of the induced acceleration model found in this study, which is comparable to previous examples mentioned earlier.

This study provides insights into the movement strategies used to achieve whole-body dynamic stability in unanticipated side cutting. Our findings reveal important non-sagittal corrective hip movements are essential to retrieve control of the CoM in the presence of otherwise excessive destabilising sagittal forces. Whilst a purely sagittal pogo stick like movement strategy may be the most efficient aim for dynamic changes of direction, this may not be possible in practice. However, practitioners looking to improve change of direction performance of their athletes may focus on the sagittal efficiency as their first priority. Reducing corrective frontal plane movement strategies may only be possible when this first priority is addressed. More holistic intervention strategies should consider an integrated approach to training and monitoring of foot placement, sagittal plane loading, and frontal plane hip engagement. In this study, we have been able to demonstrate a direct method for monitoring the necessary interlinked movement strategies and the status of whole-body dynamic stability in side cutting, which may also be applicable to other dynamic tasks.

Disclosure of funding

None.

Declaration of Competing Interest

The authors declare that no financial or personal relationship exists which may have influenced this manuscript.

Appendix A. Diagram of the laboratory set-up for the 45° unanticipated side cutting task. Cueing lights and the force plate are highlighted, the approach and change of direction paths are marked with arrows.

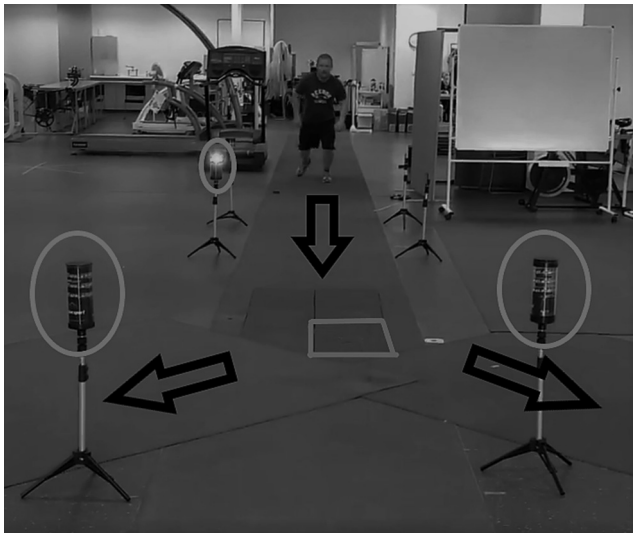

Appendix B. 0D betas for multiple regression of *foot placement* against selected side cutting performance outcomes (one subject per row).

Average M-L CoM acceleration (m/ms^{-2})	Change of direction angle (m/degrees)	Peak KAM (m/Nm kg)
1.34	−1.11	−1.94
0.25	−2.43	−2.90
−0.82	−1.07	−1.79
1.05	0.16	0.16
2.33	−1.07	−5.40
−0.72	−3.71	−3.54
1.14	−0.68	−0.22
0.31	−2.20	−0.76
−1.62	−3.23	−2.84
2.05	−2.46	−3.06
−1.13	−4.22	−0.87
1.67	−1.77	−0.37
3.49	−2.33	−0.54
2.75	−3.77	−2.85
0.50	−0.83	−1.44
1.41	−2.38	−0.23
2.36	−4.28	−1.46
0.25	−1.90	0.30
1.24	−1.39	−4.26
−0.14	−1.01	−0.05

* 'M-L' denotes medio-lateral; 'CoM' denotes centre of mass; 'KAM' denotes knee abduction moment.

References

Besier, T.F., Lloyd, D.G., Cochrane, J.L., Ackland, T.R., 2001. External loading of the knee joint during running and cutting maneuvres. Med. Sci. Sports Exerc. 33, 1168–1175.

Chen, G., 2006. Induced acceleration contributions to locomotion dynamics are not physically well defined. Gait Post. 23, 37–44.

David, S., Komnik, I., Peters, M., Funken, J., Potthast, W., 2017. Identification and risk estimation of movement strategies during cutting maneuvers. J. Sci. Med. Sport 20, 1075–1080.

Dempsey, A.R., Lloyd, D.G., Elliott, B.C., Steele, J.R., Munro, B.J., 2009. Changing sidestep cutting technique reduces knee valgus loading. Am. J. Sports Med. 37, 2194–2200.

Dempster, W.T., 1955. Space requirements of the seated operator: geometrical, kinematic, and mechanical aspects of the body with special reference to the limbs. Wright Air Development Centre Technical Report, 55–159.

Donnelly, C.J., Lloyd, D.G., Elliott, B.C., Reinbolt, J.A., 2012. Optimizing whole-body kinematics to minimize valgus knee loading during sidestepping: implications for ACL injury risk. J. Biomech. 45, 1491–1497.

Dos'Santos, T., Thomas, C., Comfort, P., Jones, P.A., 2018. The effect of angle and velocity on change of direction biomechanics: an angle-velocity trade-off. Sports Medicine 48, 2235–2253.

Hanavan, E.P., 1964. A mathematical model of the human body. Wright Air Development Centre Technical Report, 64–102.

Havens, K.L., Mukherjee, T., Finley, J.M., 2018. Analysis of biases in dynamic margins of stability introduced by the use of simplified center of mass estimates during walking and turning. Gait Post. 59, 162–167.

Havens, K.L., Sigward, S.M., 2015a. Whole body mechanics differ among running and cutting maneuvers in skilled athletes. Gait Post. 42, 240–245.

Havens, K.L., Sigward, S.M., 2015b. Joint and segmental mechanics differ between cutting maneuvers in skilled athletes. Gait Post. 41, 33–38.

Havens, K.L., Sigward, S.M., 2015c. Cutting mechanics: Relation to performance and anterior cruciate ligament injury risk. Med. Sci. Sports Exerc. 47, 818–824.

Hof, A.L., Gazendam, M.G.J., Sinke, W.E., 2005. The condition for dynamic stability. J. Biomech. 38, 1–8.

Hof, A.L., 2008. The "extrapolated center of mass" concept suggests a simple control of balance in walking. Hum. Mov. Sci. 27, 112–125.

Houck, J.R., Duncan, A., De Haven, K.E., 2006. Comparison of frontal plane trunk kinematics and hip and knee moments during anticipated and unanticipated walking and side step cutting tasks. Gait Post. 24, 314–322.

Jamison, S.T., Pan, X., Chaudhari, A.M.W., 2012. Knee moments during run-to-cut manoeuvres are associated with lateral trunk positioning. J. Biomech. 45, 1881–1885.

João, F., Veloso, A., Cabral, S., Moniz-Pereira, V., Kepple, T., 2014. Synergistic interaction between ankle and knee during hopping revealed through induced acceleration analysis. Hum. Mov. Sci. 33, 312–320.

Jones, P.A., Herrington, L.C., Graham-Smith, P., 2015. Technique determinants of knee joint loads during cutting in female soccer players. Hum. Mov. Sci. 42, 203–211.

Kepple, T.M., Siegel, K.L., Stanhope, S.J., 1997. Relative contributions of the lower extremity joint moments to forward progression and support during gait. Gait Post. 6, 1–8.

Kristianslund, E., Faul, O., Bahr, R., Myklebust, G., Krosshaug, T., 2014. Sidestep cutting technique and knee abduction loading: implications for ACL prevention exercises. Br. J. Sports Med. 48, 779–783.

Kristianslund, E., Krosshaug, T., van den Bogert, A.J., 2012. Effect of low pass filtering on joint moments from inverse dynamics: Implications for injury prevention. J. Biomech. 45, 666–671.

MacKinnon, C.D., Winter, D.A., 1993. Control of whole body balance in the frontal plane during human walking. J. Biomech. 26, 633–644.

Moniz-Pereira, V., Kepple, T.M., Cabral, S., João, F., Veloso, A.P., 2018. Joint moments' contributions to vertically accelerate the center of mass during stair ambulation in the elderly: an induced acceleration approach. J. Biomech. 79, 105–111.

Pataky, T.C., 2012. One-dimensional statistical parametric mapping in Python. Comput. Methods Biomech. Biomed. Eng. 15, 295–301.

Patla, A.E., Adkin, A., Ballard, T., 1999. Online steering: coordination and control of body center of mass, head and body reorientation. Exp. Brain Res. 129, 629–634.

Sankey, S.P., Raja Azidin, R.M.F., Robinson, M.A., Malfait, B., Deschamps, K., Verschueren, S., Staes, F., Vanrenterghem, J., 2015. How reliable are knee kinematics and kinetics during side-cutting manoeuvres? Gait Post. 41, 905–911.

Vanrenterghem, J., Gormley, D., Robinson, M.A., Lees, A., 2010. Solutions for representing the whole-body centre of mass in side cutting manoeuvres based on data that is typically available for lower limb kinematics. Gait Post. 31, 517–521.

Vanrenterghem, J., Venables, E., Pataky, T., Robinson, M.A., 2012. The effect of running speed on knee mechanical loading in females during side cutting. J. Biomech. 45, 2444–2449.

Winter, D., 1995. Human balance and posture control during standing and walking. Gait Post. 3, 193–214.